J Eng Math (2007) 58:77–90
DOI 10.1007/s10665-006-9104-8

ORIGINAL PAPER

Free-surface wave interaction with a thick flexible dock or very large floating platform

A. J. Hermans

Received: 6 February 2006/Accepted: 5 October 2006 / Published online: 15 December 2006

Abstract In this paper the recently developed semi-analytic method to solve the free-surface wave interaction with a thin elastic plate is extended to the case of a plate of finite thickness. The method used is based on the reformulation of the differential–integral equation for this problem. The thickness of the plate is chosen such that the elastic behavior of the plate can be described by means of thin-plate theory, while the water pressure at the plate is applied at finite depth. The water depth is finite.

Keywords Boundary-integral equations · Flexible platform · Free-surface flows · Hydroelasticity · Wave diffraction

1 Introduction

We consider the two-dimensional interaction of an incident wave with a flexible floating dock or very large floating platform (VLFP) with finite draft. The water depth is finite. The case of a rigid dock is a classical problem. For instance Mei and Black [1] have solved the rigid problem, by means of a variational approach. They considered a fixed bottom and fixed free-surface obstacle, so they also covered the case of small draft. After splitting the problem in a symmetric and an antisymmetric one, the method consists of matching eigenfunction expansions of the velocity potential and its normal derivative at the boundaries of two regions. In principle, their method can be extended to the flexible-platform case. Recently we derived a simpler method for both the moving rigid and the flexible dock [2]. However, we considered objects with zero draft only. In this paper we extend our approach to the case of finite, but small, draft. The draft is small compared to the length of the platform to be sure that we may use as a model, for the elastic plate, the thin-plate theory, while the water pressure at the plate is applied at finite depth. The method is based on a direct application of Green's theorem, combined with an appropriate choice of expansion functions for the potential in the fluid region outside the platform and the deflection of the plate. The integral equation obtained by Green's theorem is transformed into an integral-differential equation by making use of the equation for the elastic plate deflection. One must be careful in choosing the appropriate Green's

A. J. Hermans (✉)
Department of Applied Mathmatical Analysis, Faculty of Electrical Engineering, Mathematics and Computer Science, TU Delft, Mekelweg 4, 2628 CD Delft, The Netherlands
e-mail: a.j.hermans@ewi.tudelft.nl

function. It is crucial to use a formulation of the Green's function consisting of an integral expression only. In Appendix A we derive such a Green's function for the two-dimensional case. One may derive an expression as can be found in the article of Wehausen and Laitone [3] after application of Cauchy's residue lemma. In the three-dimensional case one also may derive such an expression. The advantage of this version of the source function is that one may work out the integration with respect to the space coordinate first and apply the residue lemma afterwards. In the case of a zero-draft platform this approach resulted in the dispersion relation in the plate region and an algebraic set of equations for the coefficients of the deflection only. Here we derive a coupled algebraic set of equations for the expansion coefficients of the potential in the fluid region and the deflection.

2 Mathematical formulation for the finite-draft problem

In this section, we derive the general formulation for the diffraction of waves by a flexible platform of general geometric form. The fluid is ideal, so we introduce a velocity potential using $\mathbf{V}(\mathbf{x},t) = \nabla\Phi(\mathbf{x},t)$, where $\mathbf{V}(\mathbf{x},t)$ is the fluid velocity vector. Hence $\Phi(\mathbf{x},t)$is a solution of the Laplace equation:

$$\Delta\Phi = 0 \quad \text{in the fluid,} \tag{1}$$

together with the linearized kinematic condition, $\Phi_z = \tilde{w}_t$, and dynamic condition, $p/\rho = -\Phi_t - g\tilde{w}$, at the mean water surface $z = 0$, where $\tilde{w}(x,y,t)$ denotes the free-surface elevation, and ρ is the density of the water. The linearized free-surface condition outside the platform, $z = 0$ and $(x,y) \in \mathcal{F}$, becomes:

$$\frac{\partial^2\Phi}{\partial t^2} + g\frac{\partial\Phi}{\partial z} = 0. \tag{2}$$

The platform is situated at the mean free surface $z = 0$, its thickness being d. The platform is modelled as an elastic plate with zero thickness. The neutral axis of the plate is at $z = 0$, while the water-pressure distribution is applied at $z = -d$. Meylan et al. [4] have considered finite thickness as well. They consider the elastic equation for the deflection of a plate of finite thickness; however, they apply the equation of motion at $z = 0$. They show for large platforms a minor influence due to the change of the elastic model. Our elastic model can easily be modified by changing the fourth-order differential operator, but due to lack of knowledge of suitable parameters we decided not to do so. So we neglect horizontal and torsional motion. To describe the vertical deflection $\tilde{w}(x,y,t)$, we apply the isotropic thin-plate theory, which leads to an equation for $\tilde{w}$ of the form:

$$m(x,y)\frac{\partial^2\tilde{w}}{\partial t^2} = -\left(\frac{\partial^2}{\partial x^2} + \frac{\partial^2}{\partial y^2}\right)\left(D(x,y)\left(\frac{\partial^2\tilde{w}}{\partial x^2} + \frac{\partial^2\tilde{w}}{\partial y^2}\right)\right) + p|_{z=-d} \tag{3}$$

where $m(x,y)$ is the piece-wise constant mass of unit area of the platform while the piece-wise constant $D(x,y)$ is its equivalent flexural rigidity. We differentiate (3) with respect to t and use the kinematic and dynamic condition to arrive at the following equation for Φ at $z = -d$ in the platform area $(x,y) \in \mathcal{P}$:

$$\left\{\left(\frac{\partial^2}{\partial x^2} + \frac{\partial^2}{\partial y^2}\right)\left(\frac{D(x,y)}{\rho g}\left(\frac{\partial^2}{\partial x^2} + \frac{\partial^2}{\partial y^2}\right)\right) + \frac{m(x,y)}{\rho g}\frac{\partial^2}{\partial t^2} + 1\right\}\frac{\partial\Phi}{\partial z} + \frac{1}{g}\frac{\partial^2\Phi}{\partial t^2} = 0. \tag{4}$$

Due to the fact that the plate is freely floating, we do not consider the hydrostatic pressure.

The edges of the platform are free of shear forces and moment. We assume that the flexural rigidity is constant along the edge and its derivative normal to the edge equals zero. Also, we assume that the radius of curvature, in the horizontal plane, of the edge is large. Hence, the edge may be considered to be straight locally. We then have the following boundary conditions at the edge:

$$\frac{\partial^2 \tilde{w}}{\partial n^2} + \nu \frac{\partial^2 \tilde{w}}{\partial s^2} = 0 \quad \text{and} \quad \frac{\partial^3 \tilde{w}}{\partial n^3} + (2-\nu)\frac{\partial^3 \tilde{w}}{\partial n \partial s^2} = 0 \tag{5}$$

where ν is Poisson's ratio, n is in the normal direction, in the horizontal plane, along the edge and s denotes the arc-length along the edge. At the bottom of the fluid region $z = -h$ we have:

$$\frac{\partial \Phi}{\partial z} = 0. \tag{6}$$

We assume that the velocity potential is a time-harmonic wave function, $\Phi(\mathbf{x}, t) = \phi(\mathbf{x})e^{-i\omega t}$. We introduce the following parameters:

$$K = \frac{\omega^2}{g}, \quad \mu = \frac{m\omega^2}{\rho g}, \quad \mathcal{D} = \frac{D}{\rho g}.$$

In a practical situation the total length L of the platform is a few thousand meters. We obtain at the free surface, $z = 0$:

$$\frac{\partial \phi}{\partial z} - K\phi = 0 \tag{7}$$

and at the plate, $z = -d$, for a single strip,

$$\left\{\mathcal{D}\left(\frac{\partial^2}{\partial x^2} + \frac{\partial^2}{\partial y^2}\right)^2 - \mu + 1\right\}\frac{\partial \phi}{\partial z} - K\phi = 0. \tag{8}$$

The potential of the undisturbed incident wave is given by

$$\phi^{\text{inc}}(\mathbf{x}) = \frac{g\zeta_\infty}{i\omega}\frac{\cosh(k_0(z+h))}{\cosh(k_0 h)}\exp\{ik_0(x\cos\beta + y\sin\beta)\}, \tag{9}$$

where ζ_∞ is the wave amplitude in the original coordinate system, ω the frequency, while the wave number k_0 is the positive real solution of the dispersion relation:

$$k_0 \tanh(k_0 h) = K, \tag{10}$$

for finite water depth. We restrict ourselves to the case of normal incidence, $\beta = 0$. In [5] it is shown that the extension to oblique waves can be done easily.

To obtain an integral equation for the deflection $\tilde{w}(x, y, t) = \mathfrak{Re}\left[w(x, y)e^{-i\omega t}\right]$ of the platform, see [6] and [5], it is very convenient to apply Green's theorem, making use of the Green's function, $\mathcal{G}(\mathbf{x}; \boldsymbol{\xi})$, that fulfills boundary conditions at the seabed (6) and at the free surface (7). Application of Green's theorem in the fluid domain leads to the following expression for the potential function:

$$4\pi\phi(\mathbf{x}) = 4\pi\phi^{\text{inc}}(\mathbf{x}) + \int_{\mathcal{C}} \phi(\boldsymbol{\xi})\frac{\partial \mathcal{G}(\mathbf{x}, \boldsymbol{\xi})}{\partial n}\, dS + \int_{\mathcal{P}} \left(\phi(\boldsymbol{\xi})\frac{\partial \mathcal{G}(\mathbf{x}, \boldsymbol{\xi})}{\partial \zeta} - \frac{\partial \phi(\boldsymbol{\xi})}{\partial \zeta}\mathcal{G}(\mathbf{x}; \boldsymbol{\xi})\right)\, dS. \tag{11}$$

The first integral is along the vertical sides of the platform, where the normal velocity of the fluid equals zero. The second integral is along the flat bottom. In the two-dimensional case, (x, z)-plane, the expression for the total potential becomes:

$$2\pi\phi(x,z) = 2\pi\phi^{\text{inc}}(x,z) + \int_{-d}^{0}\left(\phi(0,\zeta)\frac{\partial\mathcal{G}(x,z;0,\zeta)}{\partial\xi} - \phi(l,\zeta)\frac{\partial\mathcal{G}(x,z;l,\zeta)}{\partial\xi}\right)\,\mathrm{d}\zeta$$
$$+\int_{0}^{l}\left(\phi(\xi,-d)\frac{\partial\mathcal{G}(x,z;\xi,-d)}{\partial\zeta} - \frac{\partial\phi(\xi,-d)}{\partial\zeta}\mathcal{G}(x,z;\xi,-d)\right)\,\mathrm{d}\xi. \tag{12}$$

We continue with the two-dimensional case.

The Green's function $G(x, z; \xi, \zeta)$ for the two-dimensional case can be derived by means of a Fourier transform with respect to the x-coordinate. As is shown in Appendix A it has the form:

$$G(x,z;\xi,\zeta) = \int_{-\infty}^{\infty}\frac{1}{\gamma}\frac{K\,\sinh\,\gamma z+\gamma\,\cosh\,\gamma z}{K\,\cosh\,\gamma h-\gamma\,\sinh\,\gamma h}\cosh\,\gamma(\zeta+h)\mathrm{e}^{\mathrm{i}\gamma(x-\xi)}\,\mathrm{d}\gamma \quad \text{for } z>\zeta \tag{13}$$

and

$$G(x,z;\xi,\zeta) = \int_{-\infty}^{\infty}\frac{1}{\gamma}\frac{K\,\sinh\,\gamma \zeta+\gamma\,\cosh\,\gamma \zeta}{K\,\cosh\,\gamma h-\gamma\,\sinh\,\gamma h}\cosh\,\gamma(z+h)\mathrm{e}^{\mathrm{i}\gamma(x-\xi)}\,\mathrm{d}\gamma \quad \text{for } z<\zeta. \tag{14}$$

If we close the contour of integration in the complex γ-plane we obtain the complex version of formula (13.34), as can be found in [3]:

$$G(x,z;\xi,\zeta) = -2\pi\mathrm{i}\sum_{i=0}^{\infty}\frac{1}{k_i}\frac{k_i^2-K^2}{hk_i^2-hK^2+K}\cosh k_i(z+h)\cosh k_i(\zeta+h)\mathrm{e}^{\mathrm{i}k_i|x-\xi|}, \tag{15}$$

where k_0 and $k_i, i = 1, \ldots, \infty$ are the positive real and positive imaginary zeros of the dispersion relation (10).

The advantage of this formulation for Green's function is that, by means of Green's theorem, we can derive the algebraic set of equations for the expansion coefficients by carrying out the integration with respect to the spatial variable analytically first.

It is well known that for the rigid case, [1], the potential can be expanded in eigenfunctions in the regions outside and underneath the platform. In the traditional approach continuity of mass and velocity leads to sets of equations at $x = 0$ and $x = l$, respectively. The use of orthogonality relations then gives a set of equations for the unknown coefficients. In the case of zero thickness it is shown by Hermans [2] that a set of algebraic equations can be obtained for the expansion coefficients of the deflection alone. Here we also use this approach to obtain a coupled set of algebraic equations for the finite-thickness case as well. It is also possible to make a non-orthogonal expansion, see for instance [7], of the potential underneath the flexible platform. In that case one can express, a posteriori, the deflection as an expansion in exponential functions. The dispersion relations derived by both approaches are the same, as expected.

3 Semi-analytic solution

Equation 12 or the three-dimensional version (11), together with the condition at the bottom of the plate (8), can be solved by means of a numerical diffraction code based on WAMIT. However, it is interesting to see how one can solve the equations semi-analytically for simple geometries. Here we work out the case of a strip.

We eliminate in relation 12 the function $\phi(\xi,-d)$ by using Eq. 8 and the kinematic condition:

$$\phi_\zeta(\xi,-d) = -\mathrm{i}\omega w(\xi). \tag{16}$$

Thus we obtain,

$$\begin{aligned}2\pi\phi(x,z) &= 2\pi\phi^{\mathrm{inc}}(x,z) + \int_{-d}^{0}\left(\phi(0,\zeta)\frac{\partial\mathcal{G}(x,z;0,\zeta)}{\partial\xi} - \phi(l,\zeta)\frac{\partial\mathcal{G}(x,z;l,\zeta)}{\partial\xi}\right)\,\mathrm{d}\zeta\\ &\quad -\mathrm{i}\omega\int_0^l\left(\frac{1}{K}\left(\mathcal{D}\frac{\partial^4}{\partial\xi^4} - \mu + 1\right)w(\xi)\frac{\partial\mathcal{G}(x,z;\xi,-d)}{\partial\zeta} - w(\xi)\mathcal{G}(x,z;\xi,-d)\right)\mathrm{d}\xi.\end{aligned} \tag{17}$$

We assume that the deflection $w(x)$ can be written as an expansion in exponential functions, truncated at $N+2$ terms of the form:

$$w(x) = \zeta_\infty\sum_{n=0}^{N+1}\left(a_n\mathrm{e}^{\mathrm{i}\kappa_n x} + b_n\mathrm{e}^{-\mathrm{i}\kappa_n(x-l)}\right). \tag{18}$$

The values for κ_n follow from a 'dispersion' relation, yet to be determined. If we consider κ_n's with either real positive values or, if they are complex, with positive imaginary part, then the first part of expression (18) expresses modes travelling and evanescent to the right. The second part then describes modes travelling and evanescent to the left.

Furthermore, we expand the potential function for $x \le 0$ and $x \ge l$ in series of orthogonal eigenfunctions, truncated at N terms:

$$\phi(x,z) = \frac{g\zeta_\infty}{\mathrm{i}\omega}\left(\frac{\cosh\,k_0(z+h)}{\cosh\,k_0h}\mathrm{e}^{\mathrm{i}k_0x} + \sum_{n=0}^{N-1}\alpha_n\frac{\cosh\,k_n(z+h)}{\cosh\,k_nh}\mathrm{e}^{-\mathrm{i}k_nx}\right)\quad\text{for } x\le 0 \tag{19}$$

and

$$\phi(x,z) = \frac{g\zeta_\infty}{\mathrm{i}\omega}\sum_{n=0}^{N-1}\beta_n\frac{\cosh k_n(z+h)}{\cosh k_nh}\mathrm{e}^{\mathrm{i}k_n(x-l)}\quad\text{for } x\ge l, \tag{20}$$

The difference in the number of expansion functions in (18) is due to the fact that we have four boundary conditions at the edge of the plate (5). The coefficients α_0 and β_0 are the reflection and transmission coefficients, respectively. It should be noticed that the potential under the platform is *not* expanded in a set of orthogonal eigenfunctions. By the way, such a set does not exist. Extension of the solution along the bottom of the platform in the flow region is simply done by application of (17). We have introduced $4N+4$ unknown coefficients. Next we derive an algebraic set of equations for these coefficients.

First we take (x,z) at the bottom of the plate, which leads to the following equation:

$$\begin{aligned}2\pi\left(\mathcal{D}\frac{\partial^4}{\partial x^4} - \mu + 1\right)w(x) &= -2\pi\frac{K}{\mathrm{i}\omega}\phi^{\mathrm{inc}}(x,-d)\\ &\quad -\frac{K}{\mathrm{i}\omega}\int_{-d}^{0}\left(\phi(0,\zeta)\frac{\partial\mathcal{G}(x,-d;0,\zeta)}{\partial\xi} - \phi(l,\zeta)\frac{\partial\mathcal{G}(x,-d;l,\zeta)}{\partial\xi}\right)\mathrm{d}\zeta\\ &\quad +\lim_{z\uparrow -d}\int_0^l\left(\left(\mathcal{D}\frac{\partial^4}{\partial\xi^4} - \mu + 1\right)w(\xi)\frac{\partial\mathcal{G}(x,z;\xi,-d)}{\partial\zeta} - Kw(\xi)\mathcal{G}(x,z;\xi,-d)\right)\mathrm{d}\xi.\end{aligned} \tag{21}$$

We take the limit in the last integral after having carried out the spatial integrations analytically. This means that we keep the factor 2π in the left-hand side of the equation. The commonly used factor π and principle-value integral may be obtained by taking the limit first. However, it is more convenient to avoid the principle-value integral in our approach. In the first integral on the right-hand side we insert for the Green function the series expansion (15) and for the potential function the expansions (19) and (20), while in the second integral we use (14) for the Green function and (18) for the deflection. In the first integral integration with respect to ζ and in the last integral the integration with respect to ξ can be carried out. Next we close the remaining contour of integration in the complex γ-plane.

If we now equalize the coefficients of $\mathrm{e}^{\mathrm{i}\kappa_n x}$ and of $\mathrm{e}^{-\mathrm{i}\kappa_n (x-l)}$, we obtain the following 'dispersion' relation for κ_n, the κ_n's are the zero's of

$$(\mathcal{D}\kappa^4-\mu)K\cosh\kappa d+\left(K^2-\kappa^2(\mathcal{D}\kappa^4-\mu+1)\right)\frac{\sinh\kappa d}{\kappa}=(\mathcal{D}\kappa^4-\mu+1)\frac{(K\cosh\kappa h-\kappa\sinh\kappa h)}{\cosh\kappa(-d+h)}.$$

After some manipulations this relation can be rewritten in the form:

$$\left((\mathcal{D}\kappa^4-\mu-1)\kappa\tanh\kappa(h-d)-K\right)(K\sinh\kappa d-\kappa\cosh\kappa d)=0 \tag{22}$$

For $d=0$ the dispersion relation for the zero-draft platform is recovered. It should be noticed that relation (22) is not exactly the same as the zero-draft relation with h replaced by $h-d$. Hence, we ignore the zeros of the second part, that occur for values of K sufficiently large only.

3.1 Semi-infinite platform

Let us first consider the half-plane problem. We introduce some slight physical damping to get rid of the contributions of the upper bound in the last integral in (21) and the second part of the first integral. The terms we obtain after closure of the contour in the last integral of (21) contain the exponential functions $\mathrm{e}^{\mathrm{i}k_n x}$. We take the coefficients of each exponential equal to zero. This leads to a set of N algebraic equations for the coefficients a_n and α_n. For the the half-plane problem, we obtain for $i=0,\ldots,N-1$:

$$\begin{aligned}\sum_{n=0}^{N-1}\frac{\alpha_n}{\cosh k_n h}\mathcal{K}_{i,n}&-\sum_{n=0}^{N+1}\frac{a_n}{\kappa_n-k_i}\left((\mathcal{D}\kappa_n^4-\mu+1)\sinh k_i(h-d)-\frac{K}{k_i}\cosh k_i(h-d)\right)\\&=\delta_i^0\frac{hk_0^2-hK^2+K}{(k_0^2-K^2)\cosh k_0 h)}-\frac{\mathcal{K}_{i,0}}{\cosh k_0 h},\end{aligned} \tag{23}$$

where the coefficients $\mathcal{K}_{i,n}$ are defined as

$$\begin{aligned}2\mathcal{K}_{i,n}=&\frac{1}{k_i+k_n}\left[\sinh(k_i+k_n)h-\sinh(k_i+k_n)(h-d))\right]\\&+\frac{1}{k_i-k_n}\left[\sinh(k_i-k_n)h-\sinh(k_i-k_n)(h-d)\right].\end{aligned} \tag{24}$$

This is a set of N equations for $2N+2$ unknown coefficients. We have two conditions at the edge of the plate, so we must still obtain N equations. At the vertical frontend of the platform Eq. 17 gives the relation:

$$\begin{aligned}2\pi\phi(0,z)=&2\pi\phi^{\mathrm{inc}}+\lim_{x\to0}\int_{-d}^{0}\phi(0,\zeta)\frac{\partial\mathcal{G}(x,z;0,\zeta)}{\partial\xi}\,\mathrm{d}\zeta\\&-\mathrm{i}\omega\int_0^\infty\left(\frac{1}{K}\left(\mathcal{D}\frac{\partial^4}{\partial\xi^4}-\mu+1\right)w(\xi)\frac{\partial\mathcal{G}(0,z;\xi,-d)}{\partial\zeta}-w(\xi)\mathcal{G}(0,z;\xi,-d)\right)\mathrm{d}\xi.\end{aligned} \tag{25}$$

We insert the series expansions (18) and (19) in this equation and compare the coefficients of $\cosh k_i(z+h)$. For the Green function we use expression (15) in both integrals.

We obtain for $i = 0, \ldots, N-1$:

$$\frac{hk_i^2 - hK^2 + K}{(k_i^2 - K^2)\cosh\, k_i h}\alpha_i - \sum_{n=0}^{N-1} \frac{\alpha_n}{\cosh\, k_n h}\mathcal{K}_{i,n}$$
$$- \sum_{n=0}^{N+1} \frac{a_n}{\kappa_n + k_i}\left((\mathcal{D}\kappa_n^4 - \mu + 1)\sinh\, k_i(h-d) - \frac{K}{k_i}\cosh\, k_i(h-d)\right) = \frac{1}{\cosh\, k_0 h}\mathcal{K}_{i.0} \tag{26}$$

We give some results for the absolute value of the amplitude of the deflection for a semi-infinite platform with a draft of 2 m and a water depth of 10 m. In Fig. 1 results are shown for three values of the deep-water wave lengths, $\lambda = 2\pi/K = 150, 90, 30$ m, respectively. As expected, the amplitude increases with increasing values of the wave length. In Fig. 2 we show for $\lambda = 90$ m and a water depth of 10 m the absolute value of the amplitude for several values of the draft, $d = 0, 2, 4, 6$ m. In Fig. 3 we show the influence of water depth on de amplitude of deflection. We have chosen $h = 100, 20, 10$ m, $d = 2$ m and a fixed frequency with $\lambda = 90$ m. The amplitude of the deflection increases for increasing water depth. To carry out computations for the larger values of the water depth one must get rid of all hyperbolic sine and cosine functions in the formulation. This can be done by using standard formulas for these functions and by using the dispersion relation for the free-surface water waves. By doing so one obtains very accurate results. In Fig. 4 we show the real part of the deflection for the same values of water depth, $d = 5$ m, and fixed values of the wavelength, $\lambda_0 = 2\pi/k_0 = 100$ m. We have also computed the absolute value of the amplitude of the wave elevation in front of the platform. The result is shown in Fig. 5. It is clearly shown that the elevation of the wave and the platform are discontinuous at $x = 0$. The amplitude of the reflected wave $\alpha_0 = 0.45657 - 0.43639\mathrm{i}$.

3.2 Strip of finite length

We follow the same procedure as for the semi-infinite case. The first step is to compare the coefficients of the exponential functions $\mathrm{e}^{\pm \mathrm{i}k_n x}$ in (21). This leads to a set of $2N$ algebraic equations for the coefficients a_n, b_n, α_n and β_n:

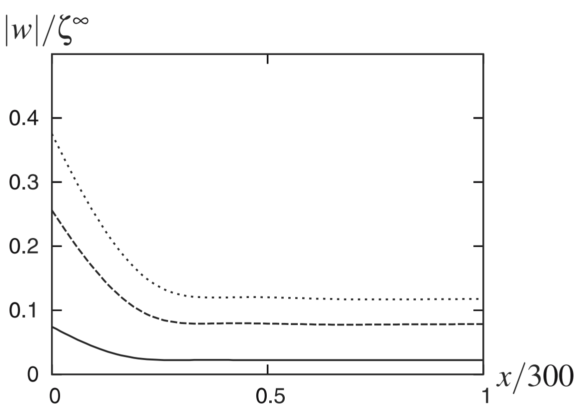

Fig. 1 $\mathcal{D} = 10^7\,\mathrm{m}^4$, $d = 2$ m, $h = 10$ m and $\lambda = 150, 90, 30$ m (top-down)

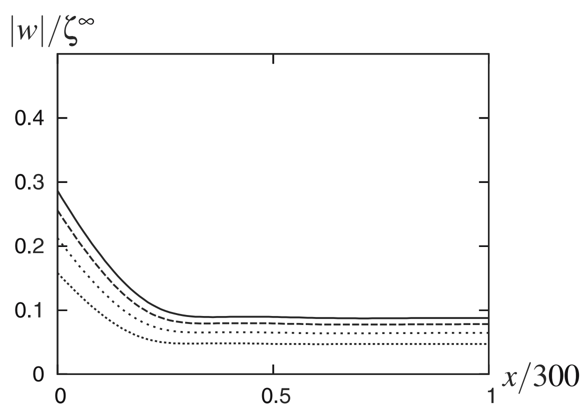

Fig. 2 $\mathcal{D} = 10^7\,\mathrm{m}^4$, $d = 0, 2, 4, 6$ m (top-down), $h = 10$ m and $\lambda = 90$ m

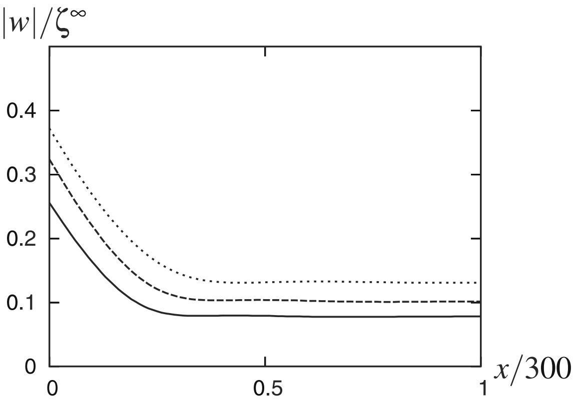

Fig. 3 $\mathcal{D} = 10^7\,\mathrm{m}^4$, $d = 2\,\mathrm{m}$, $h = 100$, 20, 10 m (top-down) and $\lambda = 90\,\mathrm{m}$

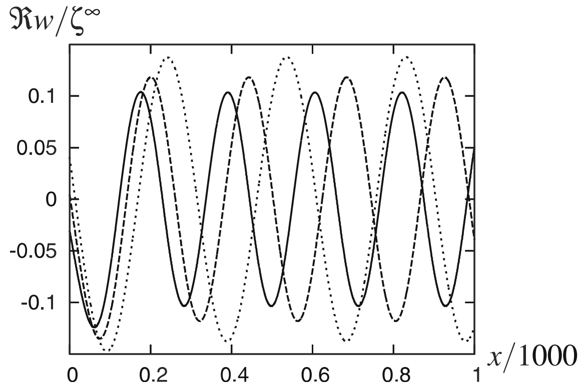

Fig. 4 Real part of the deflection for $\mathcal{D} = 10^7\,\mathrm{m}^4$, $d = 5\,\mathrm{m}$, $h = 100$, 20, 10 m (top-down) and $\lambda_0 = 100\,\mathrm{m}$

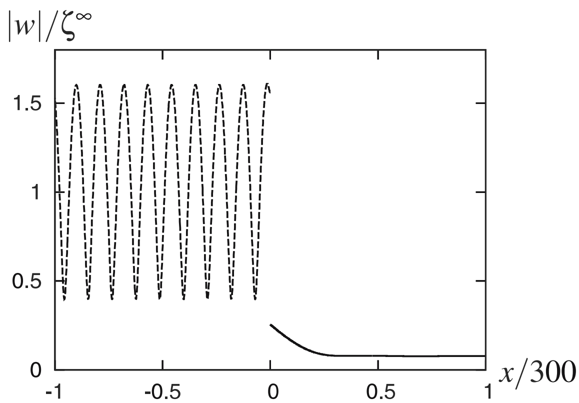

Fig. 5 Amplitude of wave and deflection for $\mathcal{D} = 10^7\,\mathrm{m}^4$, $d = 2\,\mathrm{m}$, $h = 10\,\mathrm{m}$ and $\lambda = 90\,\mathrm{m}$

$$\sum_{n=0}^{N-1} \frac{\alpha_n}{\cosh\, k_n h} \mathcal{K}_{i,n} - \sum_{n=0}^{N+1} \frac{a_n}{\kappa_n - k_i} \left((\mathcal{D}\kappa_n^4 - \mu + 1) \sinh\, k_i(h-d) - \frac{K}{k_i} \cosh\, k_i(h-d) \right)$$
$$+ \sum_{n=0}^{N+1} \frac{b_n}{\kappa_n + k_i} \left((\mathcal{D}\kappa_n^4 - \mu + 1) \sinh\, k_i(h-d) - \frac{K}{k_i} \cosh\, k_i(h-d) \right) \mathrm{e}^{\mathrm{i}\kappa_n l}$$
$$= \delta_i^0 \frac{hk_0^2 - hK^2 + K}{(k_0^2 - K^2) \cosh\, k_0 h)} - \frac{\mathcal{K}_{i,0}}{\cosh\, k_0 h} \tag{27}$$

and

$$\sum_{n=0}^{N-1} \frac{\beta_n}{\cosh\, k_n h} \mathcal{K}_{i,n} + \sum_{n=0}^{N+1} \frac{a_n}{\kappa_n + k_i} \left((\mathcal{D}\kappa_n^4 - \mu + 1) \sinh\, k_i(h-d) - \frac{K}{k_i} \cosh\, k_i(h-d) \right) \mathrm{e}^{\mathrm{i}\kappa_n l}$$
$$- \sum_{n=0}^{N+1} \frac{b_n}{\kappa_n + k_i} \left((\mathcal{D}\kappa_n^4 - \mu + 1) \sinh\, k_i(h-d) - \frac{K}{k_i} \cosh\, k_i(h-d) \right) = 0. \tag{28}$$

This is a set of $2N$ equations for $4N+4$ unknown coefficients. Next we consider the equations at $x = 0$ and $x = l$, respectively. After integration with respect to the spatial variable one obtains a summation of $\cosh k_i(z+h)$ terms. By taking the coefficients of each $\cosh k_i(z+h)$ function equal to zero we obtain the following set of $2N$ equations for the unknown expansion coefficients.

At $x = 0$ we get

$$
\begin{aligned}
&\frac{hk_i^2 - hK^2 + K}{(k_i^2 - K^2)\cosh k_i h}\alpha_i - \sum_{n=0}^{N-1} \frac{\alpha_n - \beta_n \mathrm{e}^{\mathrm{i}k_i l}}{\cosh k_n h}\mathcal{K}_{i,n} \\
&\quad - \sum_{n=0}^{N+1} \frac{a_n}{\kappa_n + k_i}\left((\mathcal{D}\kappa_n^4 - \mu + 1)\sinh k_i(h-d) - \frac{K}{k_i}\cosh k_i(h-d)\right)\left(1 - \mathrm{e}^{\mathrm{i}(\kappa_n + k_i)l}\right) \\
&\quad + \sum_{n=0}^{N+1} \frac{b_n}{\kappa_n - k_i}\left((\mathcal{D}\kappa_n^4 - \mu + 1)\sinh k_i(h-d) - \frac{K}{k_i}\cosh k_i(h-d)\right)\left(\mathrm{e}^{\mathrm{i}\kappa_n l} - \mathrm{e}^{\mathrm{i}k_i l}\right) \\
&\quad = \frac{1}{\cosh k_0 h}\mathcal{K}_{i.0},
\end{aligned}
\tag{29}
$$

and at $x = l$ we get

$$
\begin{aligned}
&\frac{hk_i^2 - hK^2 + K}{(k_i^2 - K^2)\cosh\, k_i h}\beta_i + \sum_{n=0}^{N-1} \frac{\alpha_n \mathrm{e}^{\mathrm{i}k_i l} - \beta_n}{\cosh\, k_n h}\mathcal{K}_{i,n} \\
&\quad + \sum_{n=0}^{N+1} \frac{a_n}{\kappa_n - k_i}\left((\mathcal{D}\kappa_n^4 - \mu + 1)\sinh\, k_i(h-d) - \frac{K}{k_i}\cosh\, k_i(h-d)\right)\left(\mathrm{e}^{\mathrm{i}\kappa_n l} - \mathrm{e}^{\mathrm{i}k_i l}\right) \\
&\quad - \sum_{n=0}^{N+1} \frac{b_n}{\kappa_n + k_i}\left((\mathcal{D}\kappa_n^4 - \mu + 1)\sinh\, k_i(h-d) - \frac{K}{k_i}\cosh\, k_i(h-d)\right)\left(1 - \mathrm{e}^{\mathrm{i}(\kappa_n + k_i)l}\right) \\
&\quad = \frac{hk_0^2 - hK^2 + K}{(k_0^2 - K^2)\cosh\, k_0 h}\mathrm{e}^{\mathrm{i}k_0 l} - \frac{1}{\cosh\, k_0 h}\mathcal{K}_{i.0}.
\end{aligned}
\tag{30}
$$

Together with the four relations at the end of the strip we have $4N + 4$ linear algebraic equations for the $4N + 4$ unknown coefficients.

The set of equations as it is written here is not very suitable for direct numerical computations. Especially for large values of the water-depth, the arguments of the hyperbolic sine and cosine functions become rather large. So one is subtracting very large values in the computation of the coefficients. To attain a high numerical accuracy one must get rid of these functions. This can be done by using the dispersion relation for the water region. In Appendix B a more suitable set of equations will be given.

We show some computational results for a two-dimensional platform of width 300 m. In all cases we take fixed values for the flexural rigidity $\mathcal{D} = 10^7$ m^4, the width of the strip $l = 300$ m and the water depth $h = 10$ m. In Figs. 6 and 7 we show for $d = 0$ and for $d = 2$ m the variation of the amplitude of deflection with respect to the wave length.

In Figs. 8 and 9 the dependence on the draft for fixed values of the wave length is shown. The results of the first case show an increase of the deflection for increasing values of the draft. It will be shown later that this is due to a shift in the reflection curve. In Fig. 10 a result is shown for a larger value of the flexural rigidity $\mathcal{D} = 10^{10}$ m^4 and wave length $\lambda/l = 0.5$. This case is comparable with the interaction of free-surface waves with a rigid body. One clearly observes that the motion of the dock consists of a heave and pitch motion only.

In Figs. 11 and 12 we show, for two values of the wave length, the absolute value of the amplitude of the water surface in front of and behind the strip, together with the amplitude of the plate deflection for the zero-draft case. The second case is near the zero-reflection situation.

In the 4-m-draft case, see Figs. 13 and 14, we see that $\lambda/l = 0.215$, or in terms of the actual wave length $\lambda_0/l = 0.178$, is close to total reflection. This is in contrast with the zero-draft case in Fig. 12, due to the shift in the transmission-reflection curves. For the same reason the absolute value of the deflection increases if the draft increases in Fig. 8 in contrast with the result in Fig. 9.

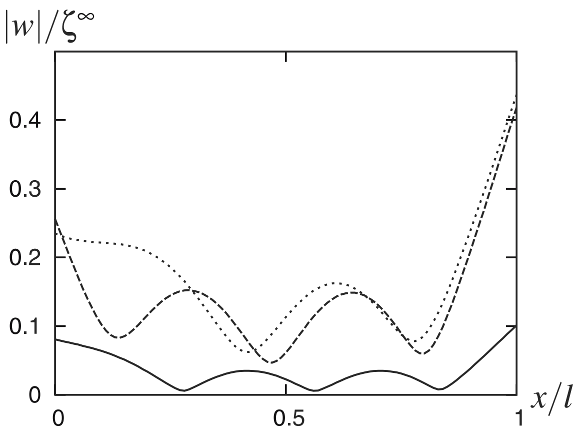

Fig. 6 $\mathcal{D} = 10^7\,\mathrm{m}^4$, $l = 300\,\mathrm{m}$, $d = 0\,\mathrm{m}$, $h = 10\,\mathrm{m}$ and $\lambda/l = 0.5, \ldots, 0.3, -- \, 0.1,$ —

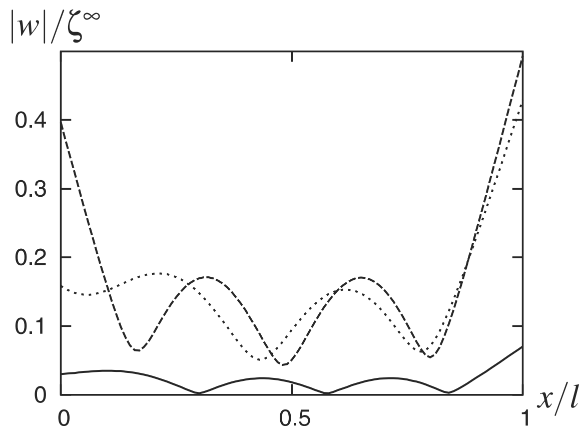

Fig. 7 $\mathcal{D} = 10^7\,\mathrm{m}^4$, $l = 300\,\mathrm{m}$, $d = 2\,\mathrm{m}$, $h = 10\,\mathrm{m}$ and $\lambda/l = 0.5,\ 0.3,\ 0.1$

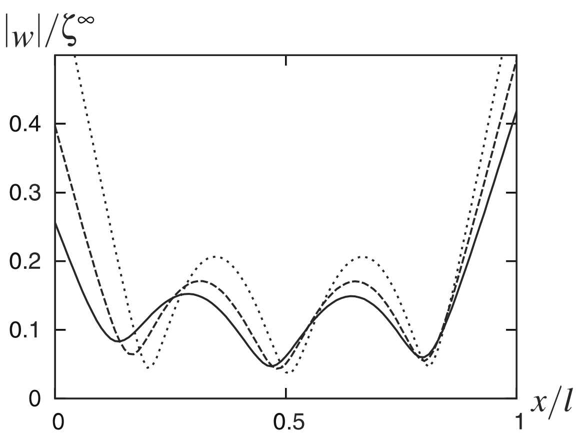

Fig. 8 $\mathcal{D} = 10^7\,\mathrm{m}^4$, $l = 300\,\mathrm{m}$, $d = 0,$ —$, 2, --, 4, \ldots\,\mathrm{m}$, $h = 10\,\mathrm{m}$ and $\lambda/l = 0.3$

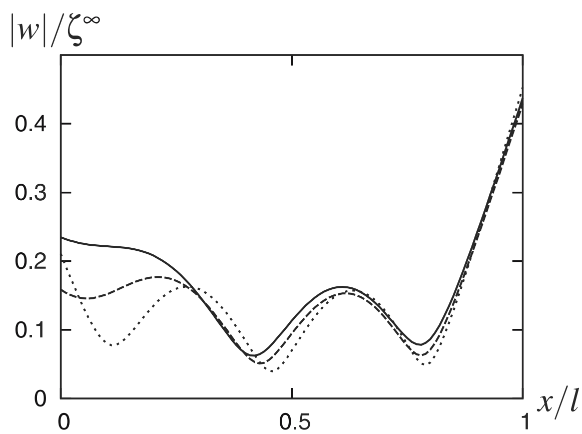

Fig. 9 $\mathcal{D} = 10^7\,\mathrm{m}^4$, $l = 300\,\mathrm{m}$, $d = 0,$ —$, 2, --, 4, \ldots\,\mathrm{m}$, $h = 10\,\mathrm{m}$ and $\lambda/l = 0.5$

Fig. 10 $\mathcal{D} = 10^{10}\,\mathrm{m}^4$, $l = 300\,\mathrm{m}$, $d = 0, 2, 4\,\mathrm{m}$, $h = 10\,\mathrm{m}$ and $\lambda/l = 0.5$

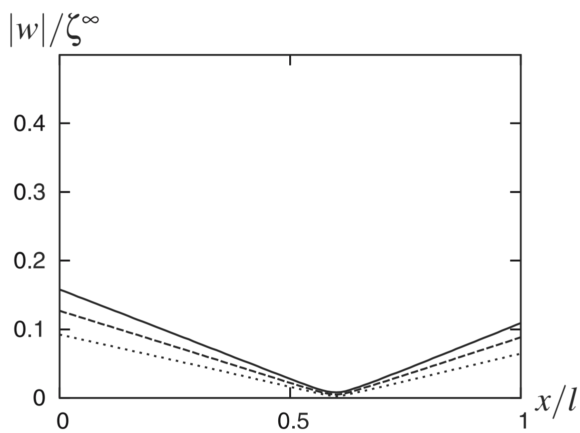

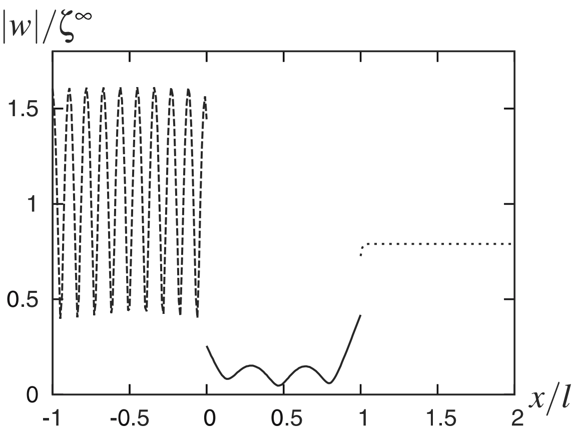

Fig. 11 $\mathcal{D} = 10^7\,\text{m}^4$, $l = 300\,\text{m}$, $d = 0\,\text{m}$, $h = 10\,\text{m}$ and $\lambda/l = 0.3$

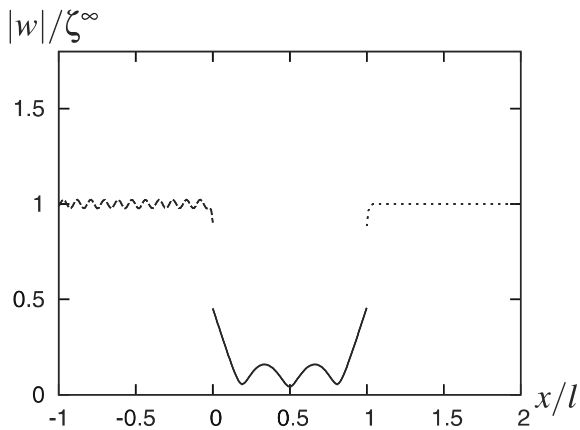

Fig. 12 $\mathcal{D} = 10^7\,\text{m}^4$, $l = 300\,\text{m}$, $d = 0\,\text{m}$, $h = 10\,\text{m}$ and $\lambda/l = 0.215$

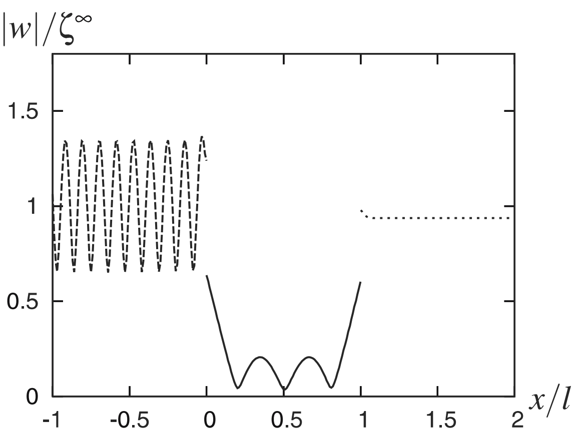

Fig. 13 $\mathcal{D} = 10^7\,\text{m}^4$, $l = 300\,\text{m}$, $d = 4\,\text{m}$, $h = 10\,\text{m}$ and $\lambda/l = 0.3$

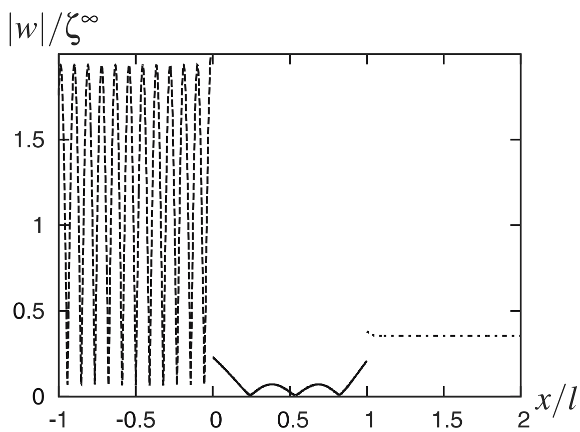

Fig. 14 $\mathcal{D} = 10^7\,\text{m}^4$, $l = 300\,\text{m}$, $d = 4\,\text{m}$, $h = 10\,\text{m}$ and $\lambda/l = 0.215$

The reflection and transmission coefficients for a strip of 300 m and depth 10 m are shown in Fig. 15, for zero-draft and in Fig. 16 for a draft of two meters. If we define $R = \alpha_0$ and $T = \beta_0$, notice no exponential function, we find that in all cases the relations $|T|^2 + |R|^2 = 1$ and $T\overline{R} + \overline{T}R = 0$ see for instance [1] or for a derivation [8], are fulfilled for at least 10 decimals. The coefficients are presented as a function of the actual wave length, $\lambda_0/l = 2\pi/k_0 l$. In the Figs. 17 and 18 these coefficients are given for a water depth of 100 m. In all cases the coefficient of flexural rigidity equals $\mathcal{D} = 10^7\,\text{m}^4$. Figures 18, 19 and 20 show the results for different sizes of the strip. In Figs. 21 and 22 the result is shown for a strip of width $l = 100\,\text{m}$ and draft $d = 8\,\text{m}$. It is clearly observed that, for the short waves, total reflection takes place.

Appendix A: The Green's function

Here we derive the two-dimensional version of the function of Green $\mathcal{G}(x, z; \xi, \zeta)$ as used in this paper. This '*source*' function is a solution of

$$\mathcal{G}_{xx} + \mathcal{G}_{zz} = 2\pi\delta(x - \xi, z - \zeta), \tag{31}$$

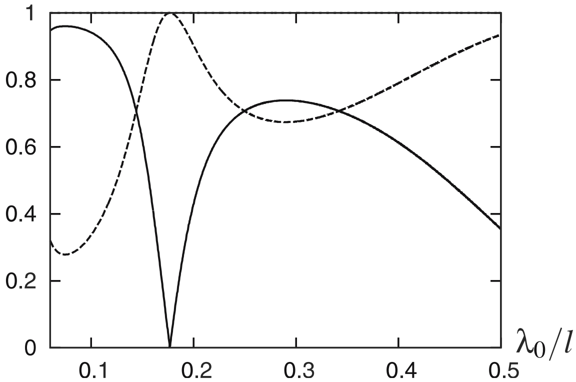

Fig. 15 —— Reflection and – – transmission coefficients for $h = 10\,\mathrm{m}$, $d = 0\,\mathrm{m}$ and $l = 300\,\mathrm{m}$

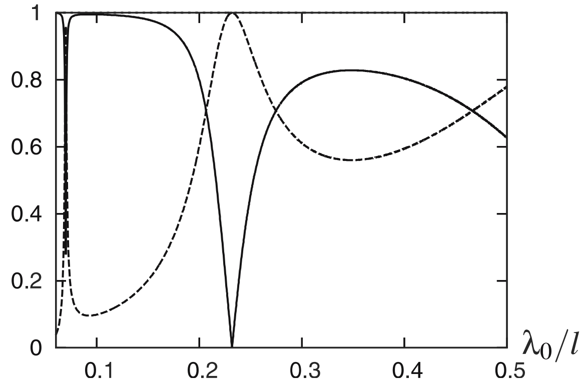

Fig. 16 Reflection and transmission coefficients for $h = 10\,\mathrm{m}$, $d = 4\,\mathrm{m}$ and $l = 300\,\mathrm{m}$

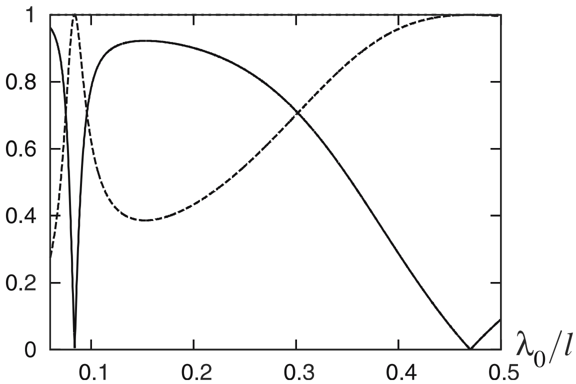

Fig. 17 Reflection and transmission coefficients for $h = 100\,\mathrm{m}$, $d = 0\,\mathrm{m}$ and $l = 300\,\mathrm{m}$

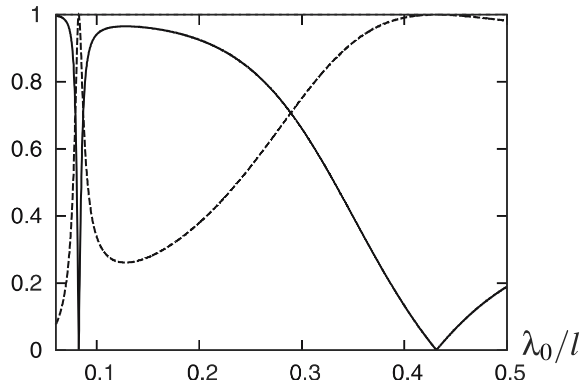

Fig. 18 Reflection and transmission coefficients for $h = 100\,\mathrm{m}$, $d = 2\,\mathrm{m}$, and $l = 300\,\mathrm{m}$

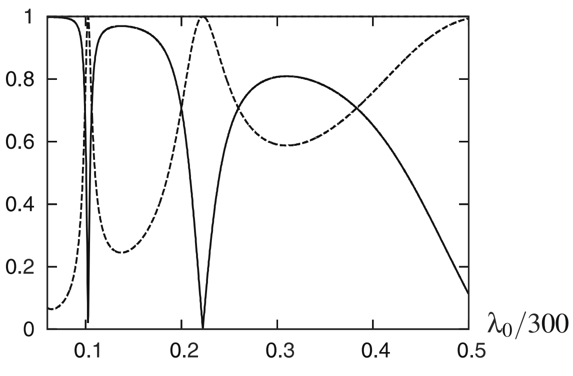

Fig. 19 Reflection and transmission coefficients for $h = 100\,\mathrm{m}$, $d = 2\,\mathrm{m}$, and $l = 650\,\mathrm{m}$

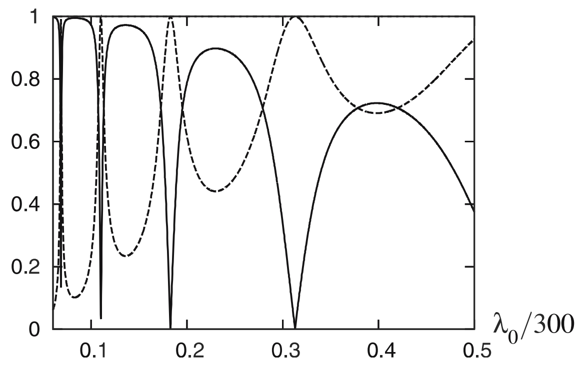

Fig. 20 Reflection and transmission coefficients for $h = 100\,\mathrm{m}$, $d = 2\,\mathrm{m}$, and $l = 1000\,\mathrm{m}$

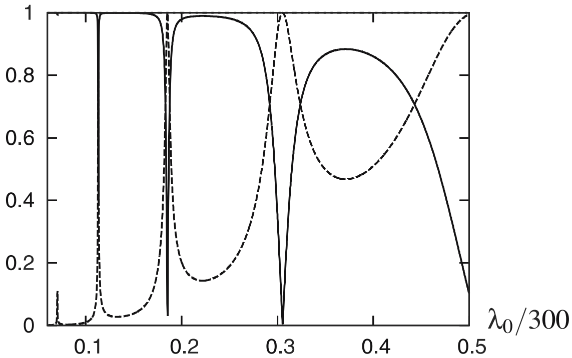

Fig. 21 Reflection and transmission coefficients for $h = 100\,\mathrm{m}$, $d = 8\,\mathrm{m}$, and $l = 1000\,\mathrm{m}$

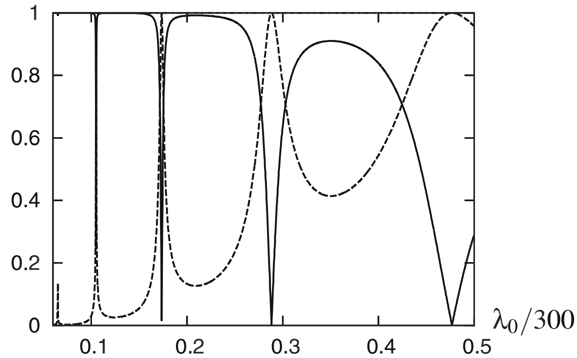

Fig. 22 Reflection and transmission coefficients for $h = 500\,\mathrm{m}$, $d = 8\,\mathrm{m}$ and $l = 1000\,\mathrm{m}$

with boundary conditions:

$$K\mathcal{G} - \mathcal{G}_z = 0 \quad \text{at } z = 0 \tag{32}$$

$$\mathcal{G}_z = 0 \quad \text{at } z = -h. \tag{33}$$

We introduce the Fourier transform of $\mathcal{G}$:

$$\tilde{\mathcal{G}}(z;\zeta) = \frac{1}{2\pi}\int_{-\infty}^{\infty} \mathcal{G}(x,z;\xi,\zeta)\mathrm{e}^{-\mathrm{i}\gamma x}\,\mathrm{d}x. \tag{34}$$

This transformed Green's function satisfies the conditions:

$$\begin{aligned}
&\tilde{\mathcal{G}}_{zz} - \gamma^2\tilde{\mathcal{G}} = 0 \quad \text{for } z \neq \zeta\\
&K\tilde{\mathcal{G}} - \tilde{\mathcal{G}} = 0 \quad \text{at } z = 0\\
&\tilde{\mathcal{G}}_z = 0 \quad \text{at } z = -h\\
&\lim_{\epsilon\to 0}\Big(\tilde{\mathcal{G}}(\zeta+\epsilon;\zeta) - \tilde{\mathcal{G}}(\zeta-\epsilon;\zeta)\Big) = 0\\
&\lim_{\epsilon\to 0}\Big(\tilde{\mathcal{G}}_z(\zeta+\epsilon;\zeta) - \tilde{\mathcal{G}}_z(\zeta-\epsilon;\zeta)\Big) = \mathrm{e}^{-\mathrm{i}\gamma\xi}.
\end{aligned} \tag{35}$$

The solution of this equations is

$$\tilde{\mathcal{G}}(z;\zeta) = \frac{1}{\gamma}\frac{K\sinh\gamma z + \gamma\cosh\gamma z}{K\cosh\gamma h - \gamma\sinh\gamma h}\cosh\gamma(\zeta+h)\mathrm{e}^{-\mathrm{i}\gamma\xi} \quad \text{for } z > \zeta \tag{36}$$

$$\tilde{\mathcal{G}}(z;\zeta) = \frac{1}{\gamma}\frac{K\sinh\gamma\zeta + \gamma\cosh\gamma\zeta}{K\cosh\gamma h - \gamma\sinh\gamma h}\cosh\gamma(z+h)\mathrm{e}^{-\mathrm{i}\gamma\xi} \quad \text{for } z < \zeta. \tag{37}$$

Then we transform back to the x-variable. This results in (13) and (14). The contour of integration passes above or underneath the singularities on the real axis. The choice of this contour is determined by the radiation condition. For $x > \xi$ the waves travel in the positive x-direction, while for $x < \xi$ the waves travel in the negative x-direction. Therefore the contour passes the negative real pole from above and the positive real pole from below. Closure of the contour in the complex γ-plane leads to (15).

Appendix B: Simplification of the set of algebraic equations

To obtain accurate solutions of the set of Eqs. 26–28 one must remove the terms that lead to subtraction of large numbers. To achieve this goal we use the dispersion relation (10), $\gamma\tanh(\gamma h) = K$. Making use of the relation:

$$\cosh(\gamma h)^2 - \sinh(\gamma h)^2 = 1,$$

one obtains for the zeros $\gamma = k_i$ for $i = 0, 1, \cdots\cdots$

$$\cosh(k_i h) = \frac{(-1)^i k_i}{\sqrt{k_i^2 - K^2}} \quad \text{and} \quad \sinh(k_i h) = \frac{(-1)^i K}{\sqrt{k_i^2 - K^2}}.$$

We also use

$$\cosh\gamma(h-d) = \cosh\,\gamma h \cosh\,\gamma d - \sinh\,\gamma h \sinh\,\gamma d$$
$$\sinh\gamma(h-d) = \sinh\,\gamma h \cosh\,\gamma d - \cosh\,\gamma h \sinh\,\gamma d.$$

One can see that for large values of the depth k_0 is very close to K and the accuracy is improved if one divides out the large term analytically. The results in Fig. 21 cannot be obtained without this simplification.

References

1. Mei CC, Black JL (1969) Scattering of surface waves by rectangular obstacles in waters of finite depth. J Fluid Mech 38:499–511
2. Hermans AJ (2003) Interaction of free-surface waves with a floating dock. J. Engng Math 45:39–53
3. Wehausen JV, Laitone EV (1960) Surface waves. Encyclopedia of physics 9. Springer-Verlag, Berlin, 446–814, also http://www.coe.berkeley.edu/SurfaceWaves/
4. Meylan MH, Squire VA (1995) The response of a thick flexible raft to ocean waves. Int Offshore Polar Eng 5:198–203
5. Hermans AJ (2003) The ray method for the deflection of a floating flexible platform in short waves. J Fluids Struct 17:593–602
6. Hermans AJ (2000) A boundary element method for the interaction of free-surface waves with a very large floating flexible platform. J Fluids Struct 14:943–956
7. Chung H, Linton CM (2003) Interaction between water waves and elastic plates: using the residue calculus technique. In: Clément AH, Ferrant P (eds) Proceedings of the 18th IWWWFB. Ecole Centrale de Nantes, France
8. Roseau M (1976) Asymptotic wave theory. North-Holland Publishing Company